XLVI CILAMCE
VITÓRIA - ES - BRAZIL - 2025
XLVI IBERO-LATIN AMERICAN CONGRESS ON COMPUTATIONAL METHODS IN ENGENEERING

Static and dynamic stability of a spherical dielectric elastomeric membrane

Suellen E. O. Alves [1], Renata M. Soares[1], Frederico M. A. da Silva[1]

[1]*School of Civil and Environmental Engineering, Federal University of Goiás*
Avenida Universitária, 1488, Qd. 86, Setor Leste Universitário, 74605-220, Goiás, Brasil
suellen@discente.ufg.br, renatasoares@ufg.br, silvafma@ufg.br

Abstract. The aim of this work is to investigate the static and the nonlinear vibration responses of an inflated spherical membrane composed of an isotropic, homogeneous, incompressible, and dielectric hyperelastic material. Both geometric nonlinearity, due to finite deformations, and material nonlinearity are considered. For the same elastomeric material, three hyperelastic constitutive models—neo-Hookean, Mooney-Rivlin, and Ogden—are employed. The system is subjected to a time-dependent uniform pressure and a continuous electric voltage to describe the nonlinear equations of motion. For each constitutive model, nonlinear static equilibrium paths, and nonlinear frequency–amplitude relationships are determined. A detailed parametric analysis highlights the significant influence of internal pressure, dielectric properties, and material parameters on the static stability and nonlinear oscillations of the membrane, revealing the emergence of distinct structural stability regimes depending on the chosen constitutive model.

Keywords: spherical membrane, dielectric elastomer, dynamic stability.

1 Introduction

Hyperelastic materials are characterized by the possibility of undergoing large reversible deformations and presenting nonlinear behavior. These mechanical properties can be internal electrical properties that add new fields of action for these materials. In this context, the use of structures, such as plates, shells and membranes, composed of dielectric elastomers has become more common [1-5], which increases the need to understand their nonlinear behavior. Their use can be observed in several areas of engineering, such as robotics (light and industrial robots), biological devices, actuators, and energy harvesters [6-8].

The constitutive models of dielectric elastomeric materials are described through the deformation energy density functions and the neo-Hookean, Mooney-Rivlin and Ogden models are examples of representation of this type of materials [2-4, 9]. And, some researchers have studied the static and dynamic behavior of dielectric hyperelastic membranes and shells, with emphasis on spherical geometry, investigating the influence of pre-stressing, internal and external pressure, oscillations and stability [2-4, 10-11].

Zhu *et al* [2] studied the dynamic behavior of a dielectric elastomer balloon subject to a combination of pressure and voltage. The authors determined the stability of the state of equilibrium and calculated the natural frequency of the small-amplitude oscillation around the state of equilibrium with focus on the parametric responses of the dielectric elastomer balloon. When the voltage is sinusoidal, the balloon resonates at multiple frequencies of excitation, giving rise to superharmonic, harmonic and subharmonic responses. When the frequency of excitation varies continuously, the oscillating amplitude of the balloon may jump, exhibiting hysteresis.

Tang *et al* [4] investigated the nonlinear vibrations of the spherical shell characterized by the Ogden model with structural damping, pressure, direct current voltage and alternating current voltage. The governing equation describing the radially symmetric motions of the shell is derived by the incompressibility constraint and the variational method. It is shown that with the increasing pressure and voltage, the vibrations transition from periodic vibrations to chaotic vibrations

This paper analyzes investigate the static and the nonlinear vibration responses of an inflated spherical

membrane composed of an isotropic, homogeneous, incompressible, and dielectric hyperelastic material. Both geometric nonlinearity, due to finite deformations, and material nonlinearity are considered. For the same elastomeric material, three hyperelastic constitutive models—neo-Hookean, Mooney-Rivlin, and Ogden—are employed. The nonlinear static equilibrium paths and nonlinear frequency–amplitude relationships are determined. A detailed parametric analysis highlights the significant influence of internal pressure, dielectric properties, and material parameters on the static stability and nonlinear oscillations of the spherical membrane.

2 Mathematical formulation

Consider the spherical membrane of initial radius a, thickness h, density γ and composed of dielectric hyperelastic material. It is assumed that $h/a << 1$ such that the deformed membrane can be described by the theory of thin-walled membranes under finite deformations. Let P be a point on the undeformed middle surface in the coordinate system (r, s, θ) that moves to P' (x, y, θ) after deformation at a time t as shown in Fig. 1 [9].

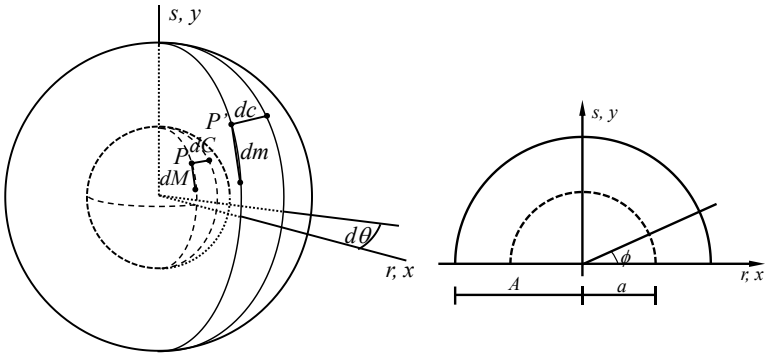


Figure 1. Axisymmetric undeformed (dashed lines) and deformed (continuous lines) configurations of the spherical membrane and associated coordinate systems [9].

Considering the meridional and circumferential infinitesimal elements adjacent to P in the undeformed configuration (dM, dC) and to P' in the deformed configuration (dm, dc) and the definition of the principal stretches as $\lambda_i = ds_i / dS_i$, where dS_i and ds_i are the undeformed and deformed lengths, respectively, the principal stretches λ_1 and λ_2 of the spherical membrane can be written as (see Fig. 1) [9].

$$\lambda_1 = \frac{dm}{dM} = \frac{A(t)}{a} \quad \lambda_2 = \frac{dc}{dC} = \frac{A(t)}{a} \tag{1}$$

where $A(t) = A_1 + A_2 \cos(\omega t)$ represents the time-dependent radius of the membrane in the deformed configuration. Due to the incompressibility constraint ($I_3 = 1$), the principal stretch in the radial direction is given by

$$\lambda_3 = \frac{1}{\lambda_1 \lambda_2} = \left(\frac{a}{A(t)}\right)^2 \tag{2}$$

Dielectric hyperelastic materials are described under the assumption of the existence of a strain energy density function per unit volume W. The strain energy density function W can be written as a function of the strain invariant $I_i(\lambda_i)$ Here, three hyperelastic incompressible constitutive models—neo-Hookean, Mooney-Rivlin, and Ogden—are adopted. The Mooney-Rivlin model assumes the following form (eq (3)):

$$W = C_1[(I_1 - 3) + \alpha(I_2 - 3)] + \frac{D^2}{2\varepsilon} \tag{3}$$

where $\alpha = C_2/C_1$, with C_1 and C_2 are material constants, ε is the dielectric constant of elastomer, and $D = \varepsilon E$ is the electric displacement associated with the electric field E. If $\alpha = 0$, the neo-Hookean constitutive model is obtained as a special case of the Mooney– Rivlin model.

The Ogden material model assumes that the material behavior can be described by means of a strain-energy density function given by eq (4):

$$W = \sum_{i=1}^{N} \frac{\mu_i}{\alpha_i} \left(\lambda_1^{\alpha i} + \lambda_2^{\alpha i} + \lambda_3^{\alpha i} - 3\right) + \frac{D^2}{2\varepsilon} \tag{4}$$

where N is the number of terms of function and α_i are material constants.

According to [4], the electric field E is given by eq (5):

$$E = \frac{\lambda^2 V}{h} \tag{5}$$

where λ is used to describe the stretch ratio and V is the voltage applied at the membrane.

The elastic strain energy of the membrane U is defined as the volume integral of W in the undeformed configuration:

$$U = 2\pi h a^2 \int_0^{\frac{\pi}{2}} \cos(\phi) W \, d\phi \tag{6}$$

The work performed by radially distributed pressure $p(t)$ on the inner surface of the membrane is defined as the product of the applied pressure and the variation of the volume enclosed by the membrane [9] and is given by:

$$W_k = p(t)\pi[A(t)^3 - a^3] \int_0^{\frac{\pi}{2}} \cos\phi^3 \, d\phi \tag{7}$$

and the work done by the voltage V is:

$$W_v = 2\pi h a^2 \int_0^{\frac{\pi}{2}} \cos\phi \varepsilon \left(\frac{V}{h}\right)^2 (\lambda_1 \lambda_2)^2 \, d\phi \tag{8}$$

The kinetic energy T is given by

$$T = \pi a^4 h \, \gamma \dot{A}(t)^2 \tag{9}$$

where $\dot{(\ )} = d(\ )/dt$.

In order to obtain the governing equation of the membrane, the Euler–Lagrange equation is introduced in the Lagrangean defined by:

$$L = T - U + W_k + W_v \tag{10}$$

In the static formulation, the dependence of the time (t) is disregarded, therefore the kinetic energy in the Lagrangian is neglected. The total potential energy (Π) in function of the static uniform pressure is considered. By applying the minimum potential energy criterion ($d\Pi/dA=0$), the nonlinear equilibrium equation of the membrane under uniform internal pressure is obtained. Introducing the nondimensional variables:

$$\bar{P_1} = \frac{a p_1}{h C_1} \qquad \overline{P_2} = \frac{a p_2}{h C_1} \tag{11}$$

$$\bar{V} = \frac{\varepsilon V^2}{C_1 h^2} \tag{12}$$

$$\delta = \frac{A_1}{a} \tag{13}$$

the nondimensional uniform internal pressure ($\bar{P_1}$) and nondimensional voltage ($\bar{V}$), considering the Mooney-Rivlin model (eq (3)), can be written as:

$$\bar{P_1} = 4(\delta\alpha - \delta^{-5}\alpha + \delta - \delta^{-7}) - 2\delta\bar{V} \tag{14}$$

If $\alpha = 0$, we obtain the equations for the neo-Hookean constitutive model. Considering the Ogden constitutive model (eq (4)), with $N = 3$, we have the equations for the nondimensional uniform internal pressure ($\bar{P}$) and nondimensional voltage ($\bar{V}$):

$$\bar{P_1} = \frac{2}{C_1}\left[\mu_1\left(\delta^{\alpha_1 - 3} - \frac{1}{\delta^{3+2\alpha_1}}\right) + \mu_2\left(\delta^{\alpha_2 - 3} - \frac{1}{\delta^{3+2\alpha_2}}\right) + \mu_3\left(\delta^{\alpha_3 - 3} - \frac{1}{\delta^{3+2\alpha_3}}\right)\right] - 2\delta\bar{V} \tag{15}$$

For dynamic analysis, Hamilton's principle is applied to the Lagrangian, and since it is a non-conservative system, the damping term is included in the equation of motion $R_e = 2\zeta\omega_o a^2 h \, \gamma \dot{A}(t)$. The preloaded membrane is then subjected to a time-varying pressure given by:

$$p(t) = \bar{P_1} + \overline{P_2}\cos(\Omega t) \tag{16}$$

composed of a static portion, $\bar{P_1}$, and a dynamic portion, where $\overline{P_2}$ represents the amplitude of the dynamic portion of the pressure. The ratio $\Omega = \omega_f / \omega_o$ is defined, where ω_f is the excitation frequency of the dynamic load and ω_o is the natural frequency of the membrane.

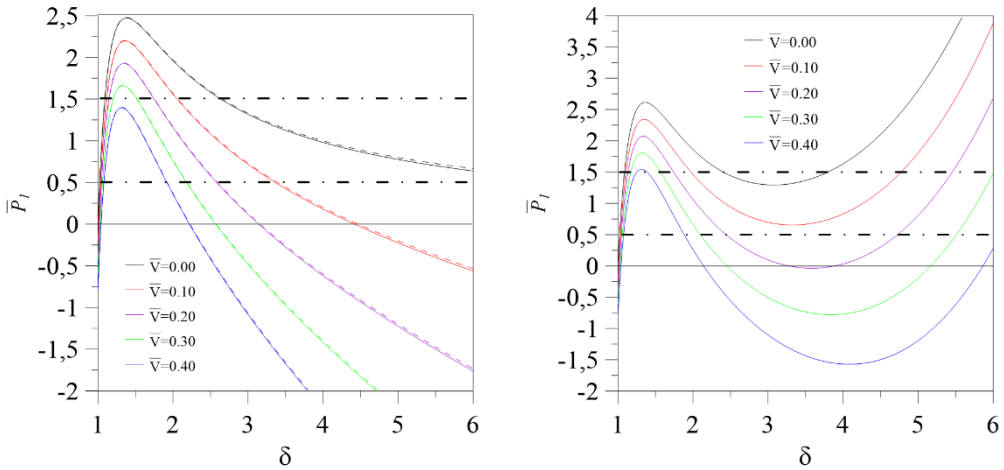
3 Numerical Results

A dielectric hyperelastic spherical membrane of radius $a = 1m$, thickness $h = 0.001m$, and density $\gamma = 1100\ kg/m^3$ is considered. The parameters used in the constitutive models are presented in Tab 1 [12].

Table 1. Parameters in constitutive models

Constitutive Model	Values
neo-Hookean	$C_1 = 0.208$ MPa $\alpha = 0$
Mooney-Rivlin	$C_1 = 0.208$ MPa $\alpha = -0.0012$
Ogden	$\mu_1 = 161.2$ Pa $\mu_2 = -1831$ Pa $\mu_3 = 781.1$ kPa $\alpha_1 = 7.295$ $\alpha_2 = -2.729$ $\alpha_3 = 1.056$

Figure 2 presents the results obtained for the uniform internal pressure ($\bar{P}_1$) *versus* the stretch ratio (δ) with different nondimensional voltages values ($\bar{V}$). In Fig. 2a the dashed lines represent the results considering the neo-Hookean model and the solid lines the Mooney Rivlin model (eq. 14), while Fig. 2b shows the results considering the Ogden model (eq 15). As illustrated in Fig. 2a, the neo-Hookean and Mooney-Rivlin models yield the same nonlinear static equilibrium path, exhibiting a quasi-linear behavior up to the limit point of the applied pressure $\bar{P}_1$. This limit point decreases as the nondimensional voltage parameter increases. Beyond the limit point, the spherical membrane experiences a reduction in pressure with increasing stretch ratio, and this reduction becomes more pronounced at higher values of $\bar{V}$.



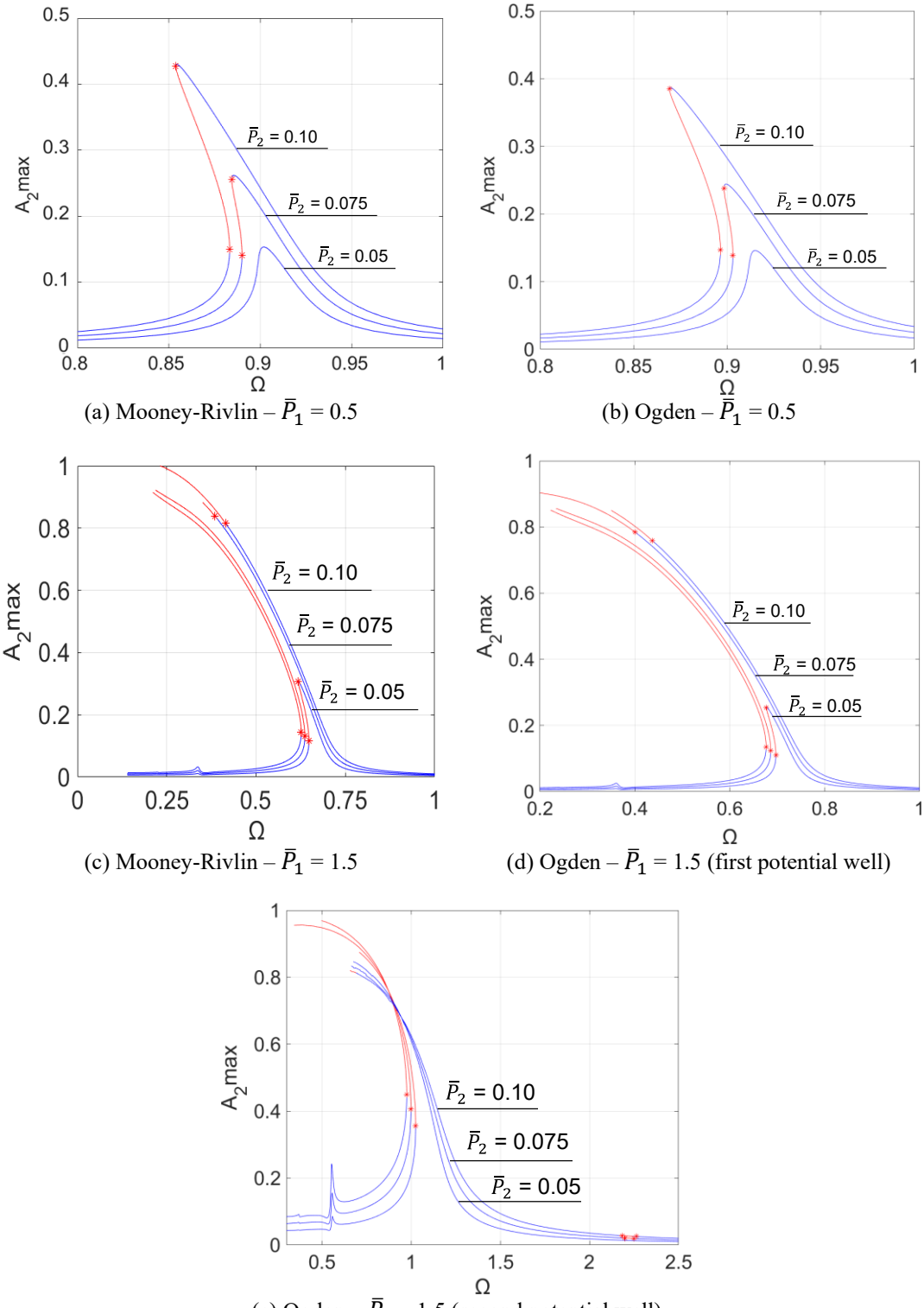
(a) neo-Hookeano e Mooney-Rivlin (b) Ogden

Figure 2 Uniform internal pressure ($\bar{P}_1$) *versus* stretch ratio (δ) (a) neo-Hookean (– –) and Mooney-Rivlin (——) (b) Ogden.

On the other hand, in the Ogden model, Fig. 2b, lower critical voltage values are again observed for higher applied voltages. However, differently from the previously considered models, the membrane exhibits a stiffness gain, i.e., an increase in internal pressure with increasing radial stretch is observed after reaching a minimum pressure point.

After studying the influence of static pressure and voltage on the membrane responses, a forced vibration analysis is performed, considering the internal pressure with static and dynamic terms according to eq. (16). Thus, the resonance curves are obtained only for the Mooney-Rivlin and Ogden models, since the responses considering the neo-Hookean model are very similar to those of the Mooney-Rivlin model. For this purpose, from Fig. 2, it is considered the following parameters: $\bar{V} = 0.1$ (red curve) and two pre-static pressure, $\bar{P}_1 = 0.5$ and $\bar{P}_1 = 1.5$ (horizontal lines – · –), to investigate the nonlinear dynamic equilibrium when a time-dependent pressures acts in the spherical membrane. In the next results, the linear viscous damping coefficient is $\zeta = 0.01$.

The resonance curves were obtained using the continuation package for dynamical analysis MatCont [13] for both the Mooney-Rivlin and Ogden models, as shown in Fig. 3. In this figure, the blue lines represent stable branches, while the red lines indicate unstable branches.



(a) Mooney-Rivlin – $\bar{P}_1 = 0.5$

(b) Ogden – $\bar{P}_1 = 0.5$

(c) Mooney-Rivlin – $\bar{P}_1 = 1.5$

(d) Ogden – $\bar{P}_1 = 1.5$ (first potential well)

(e) Ogden – $\bar{P}_1 = 1.5$ (second potential well)

Figure 3 Resonance curves for spherical membrane described by (a, c) Mooney-Rivlin and (b, d, e) Ogden constitutive laws for the following pre-static pressure: (a, b) $\bar{P}_1 = 0.5$ and (c-e) $\bar{P}_1 = 1.5$.

As observed in Figs. 3a and 3b, both constitutive models exhibit similar softening resonance curves as the excitation pressure amplitude $\overline{P_2}$ increases, with the maximum resonance peak being slightly higher for the Mooney-Rivlin model (Fig. 3a). As $\overline{P_2}$ increases, the resonance curves evolve from a quasi-linear profile, featuring a resonance peak near the membrane's natural frequency, into a nonlinear response characterized by two saddle-node bifurcation points that define the unstable branch. According to Fig. 2, the pre-static pressure $\bar{P}_1 = 0.5$ intersects the nonlinear equilibrium path only within the first potential well, which is associated with low vibration amplitudes under the excitation pressure amplitudes investigated.

By increasing the value of $\bar{P}_1$ to 1.5, it can be observed from Fig. 2b that this value intersects the nonlinear static equilibrium curve of the Ogden model at two points. The second intersection, around $\delta = 4.8$, corresponds to the second potential well. In contrast, for the Mooney-Rivlin model, this value of $\bar{P}_1$ continues to intersect only the stable branch of the nonlinear static equilibrium curve. As shown in Figs. 3c and 3d, within the first potential well, both constitutive models exhibit very similar resonance curves. The Mooney-Rivlin model (Fig. 3c) presents slightly higher vibration amplitudes compared to the Ogden model (Fig. 3d). It is important to highlight that, since $\bar{P}_1$ is close to the limit point of stability loss, the excitation amplitudes $\overline{P_2} = 0.075$ and $\overline{P_2} = 0.1$ result in split resonance curves characterized by an extended unstable branch. This behavior indicates a divergence in the dynamic response for the Mooney-Rivlin model, or a dynamic jump to a new stable branch (associated with the secondary potential well) in the case of the Ogden model.

Figure 3e shows the resonance curves obtained for the Ogden model in the second potential well, considering different excitation amplitudes. In this figure, the resonance peak occurs at an excitation frequency of approximately 1.1. As expected, the natural frequency of the spherical membrane in the second potential well is higher than that in the first potential well. Consequently, the resonance curves in Fig. 3e are shifted to the right compared to those in Fig. 3d.

4 Conclusions

In this work, the static and vibration nonlinear response of an inflated spherical membrane composed of a dielectric hyperelastic material were investigated. To obtain the governing equations, geometric and physical nonlinearities are considered in a system subjected to time-dependent uniform pressure and a continuous electric voltage.

The neo-Hookean and Mooney-Rivlin models yield the same nonlinear static equilibrium path, exhibiting a quasi-linear behavior up to the limit point of the applied pressure. This limit point decreases as the nondimensional voltage parameter increases. However, in the Ogden model the membrane exhibits a stiffness gain after reaching a minimum pressure point. For Ogden and Mooney-Rivlin models, the resonance curves exhibit softening behavior when the excitation pressure amplitude $\overline{P_2}$ increases. The Ogden model shows a second potential well in the resonance curves with higher natural frequencies than that in the first potential well.

Acknowledgements. The authors are grateful for the financial support provided by CAPES, CNPq and FAPEG for the development of this work.

Authorship statement. The authors hereby confirm that they are the sole liable persons responsible for the authorship of this work, and that all material that has been herein included as part of the present paper is either the property (and authorship) of the authors, or has the permission of the owners to be included here.

References

[1] N. C. Goulbourne; E.M. Mockensturm; M. I. Frecker, “Electro-elastomers: large deformation analysis of silicone membranes”, *Int. J. Solids Struct.*, vol 44, pp 2609–2626, 2007

[2] J. Zhu; S. Cai; Z. Suo, “Resonant behavior of a membrane of a dielectric elastomer”. *International Journal of Solids and Structures*, vol 47, pp 3254-3262, 2010.

[3] H. Yong; X. He; Y. Zhou, “Dynamics of a thick-walled dielectric elastomer spherical shell”. *International Journal of Engineering Science,* vol 49, pp792-800, 2011.

[4] Y. Tang; X. Yuan; Z. Zhao; R. Wang; Z. Wang, "Periodic and chaotic vibrations of dielectric elastomer spherical shells considering structural damping", *Nonlinear Dynamic*, vol 113, pp 1025–1040, 2024.
[5] A. Mishra, Y. S. Joshan, S. K. Wahi, S. Santapuri, "Structural instabilities in soft electro-magneto-elastic cylindrical membranes", *International Journal of Non-Linear Mechanics*, vol 151, 2023.
[6] N. Goulbourne, E. Mockensturm, M. Frecker, "A Nonlinear Model for Dielectric Elastomer Membranes." *J. Appl. Mech*., vol 72, pp 899–906, 2005.
[7] F. Carpi, D.D. Rossi, R. Kornbluh, R. Pelrine, P. Sommer-Larsen, *Dielectric Elastomers as Electromechanical Transducers: Fundamentals, Materials, Devices, Models and Applications of an Emerging Electroactive Polymer Technology*. Elsevier, 2008.
[8] D.D. Tommasi, G. Puglisi, G. Saccomandi, G. Zurlo, "Pull-in and wrinkling instabilities of electroactive dielectric actuators", *Journal of Physics D –Applied Physics*, vol 43, 2010.
[9] R.M. Soares, P.F.T. Amaral, F.M.A. Silva, P. B. Gonçalves, "Nonlinear breathing motions and instabilities of a pressure-loaded spherical hyperelastic membrane" *Nonlinear Dynamic*, vol 99, pp 351–372, 2020.
[10] X.LV, L. LIU, Y, LIU, J. LENG, "Dynamic performance of dielectric elastomer balloon incorporating stiffening and damping effect", *Smart Mater. Struct.* vol 27, 2018.
[11] X. JIN, Y. WANG, M.Z. CHEN, Z. HUANG, "Response analysis of dielectric elastomer spherical membrane to harmonic voltage and random pressure", *Smart Mater. Struct.*, vol 26, 2017.
[12] I. D. Breslavsky, M. Amabili, M. Legrand, "Nonlinear vibrations of thin hyperelastic plates", *Journal of Sound and Vibration*, vol 333, pp 4668-4681, 2014.
[13] W. Govaerts, Y. A. Kuznetsov, and H. G. Meijer. MatCont Numerical Bifurcation Analysis Toolbox in Matlab, version 2021 (matcont7p3).